BIOCHEMISTRY
including biophysical chemistry & molecular biology
Article

Biochemistry **2009,** *48,* 3853–3863 3853
DOI:10.1021/bi802371h

A Two-Step Binding Model Proposed for the Electrostatic Interactions of Ricin A Chain with Ribosomes[†]

Xiao-Ping Li,[‡] Jia-Chi Chiou,[‡] Miguel Remacha,[§] Juan P. G. Ballesta,[§] and Nilgun E. Tumer*[,‡]

[‡]*Biotechnology Center for the Agriculture and the Environment, School of Environmental and Biological Sciences, Rutgers University, New Brunswick, New Jersey 08901-8520, and* [§]*Centro de Biología Molecular Severo Ochoa, Consejo Superior de Investigaciones Científicas and Universidad Autónoma de Madrid, 28049 Madrid, Spain*

Received December 30, 2008. Revised Manuscript Received February 20, 2009

ABSTRACT: Ricin is a ribosome inactivating protein that catalytically removes a universally conserved adenine from the α-sarcin/ricin loop (SRL) of the 28S rRNA. We recently showed that ricin A chain (RTA) interacts with the P1 and P2 proteins of the ribosomal stalk to depurinate the SRL in yeast. Here we examined the interaction of RTA with wild-type and mutant yeast ribosomes deleted in the stalk proteins by surface plasmon resonance. The interaction between RTA and wild-type ribosomes did not follow a single-step binding model but was best characterized by two distinct types of interactions. The AB1 interaction had very fast association and dissociation rates, was saturable, and required an intact stalk, while the AB2 interaction had slower association and dissociation rates, was not saturable, and did not require the stalk. RTA interacted with the mutant ribosomes by a single type of interaction, which was similar to the AB2 interaction with the wild-type ribosomes. Both interactions were dominated by electrostatic interactions, and the AB1 interaction was stronger than the AB2 interaction. On the basis of these results, we propose a two-step interaction model. The slow and ribosomal stalk nonspecific AB2 interactions concentrate the RTA molecules on the surface of the ribosome. The AB2 interactions facilitate the diffusion of RTA toward the stalk and promote the faster, more specific AB1 interactions with the ribosomal stalk. The electrostatic AB1 and AB2 interactions work together allowing RTA to depurinate the SRL at a much higher rate on the intact ribosomes than on the naked 28S rRNA.

Ricin is a ribosome inactivating protein (RIP)[1] isolated from the castor bean plant, *Ricinus communis*, that consists of a ricin toxin A chain (RTA) and a galactose-binding B chain (RTB). RTA and RTB are linked by a disulfide bond between Cys 259 near the C-terminus of RTA and Cys 4 of RTB (*1*). The holotoxin is not active on ribosomes (*2*−*6*). The enzymatic activity of ricin is due to RTA, which is an *N*-glycosidase that specifically cleaves the *N*-glycosidic bond at A4324 of the 28S rRNA of rat ribosomes (*7*) and inhibits the elongation factor-dependent ribosomal functions (*8*−*10*). RTA can also cleave the A2660 in naked 23S rRNA from *Escherichia coli* but not the ribosomes from *E. coli* (*11*−*14*). Both A4324 of rat 28S rRNA and A2660 of *E. coli* 23S rRNA are located at a universally conserved rRNA stem loop called the α-sarcin/ricin loop (SRL) named after the toxins (*9*). The SRL is the site where elongation factors interact with the ribosome and is involved in peptide translocation during protein synthesis (*15*). RTA depurinates the 28S rRNA on rat ribosomes ~5000 times faster than the naked rat 28S rRNA (*7*), indicating that the conformation of the rRNA on intact ribosomes and the ribosomal proteins play an important role in ribosome depurination by ricin.

The α-sarcin/ricin loop (SRL) is located on the 60S subunit in the proximity of the ribosomal stalk, which is a lateral flexible structure on the large subunit. The stalk region was not resolved on the structure of the bacterial ribosome at 3.5 Å resolution because of its mobility (*16*). Biochemical studies have shown that the ribosomal stalk is composed of an rRNA binding protein, which is L10 in prokaryotic ribosomes and P0 in eukaryotic ribosomes together with two to three pairs of L7/L12 heterodimer in bacteria and P1/P2 heterodimer in eukaryotic ribosomes (*17*). The N-termini of L7/L12 proteins directly interact

[†]This work was supported by National Institutes of Health Grant AI072425 (to N.E.T.) and Grant BFU2006-00365 from Ministerio de Educacion y Ciencia (to J.P.G.B.).

*To whom correspondence should be addressed: Biotechnology Center for the Agriculture and the Environment, School of Environmental and Biological Sciences, Rutgers University, 59 Dudley Rd., New Brunswick, NJ 08901-8520. Phone: (732) 932-8165, ext. 215. Fax: (732) 932-6535. E-mail: tumer@aesop.rutgers.edu.

[1]Abbreviations: RTA, ricin A chain; RTB, ricin B chain; PAP, pokeweed antiviral protein; TCS, trichosanthin; Stx1, Shiga-like toxin 1; SRL, α-sarcin/ricin loop; SPR, surface plasmon resonance; RIP, ribosome inactivating protein; NTD, N-terminal domain; CTD, C-terminal domain; EGFP, enhanced green fluorescent protein; RU, resonance unit; eEF2, eukaryotic elongation factor 2.

Published on Web 3/18/2009

with L10, which interacts with the rRNA through its N-terminal domain (*18*,*19*). The L7/L12 heterodimer is involved in factor recruitment and factor-dependent GTP hydrolysis (*17*,*20*,*21*). Because of the difficulty in resolving the stalk structure on the intact ribosome, the crystal structure of L10 together with the L7/L12 N-terminal domain (NTD) from *Thermotoga maritime* was determined (*22*). Using these data together with the crystal structure of the 70S subunit from *E. coli*, a functional model was proposed (*22*). According to this model, multiple copies of the C-termini of the stalk proteins exposed to the cytosol recruit the translation factors and deliver them to the SRL on the ribosome in the right conformation through the flexible hinge of the stalk proteins. This model explained the two well-known observations during protein synthesis, the dynamic conformational change of the stalk and the high rate of translation factor binding to the ribosomes.

We have shown that pokeweed antiviral protein (PAP), one of the type I RIPs, interacts with the yeast ribosomal protein L3 to depurinate the SRL (*23*). The importance of this interaction was further confirmed by other researchers (*24*). Chemical cross-linking experiments showed that RTA interacted with L9 and L10e (P0) on mammalian ribosomes (*25*). Trichosanthin (TCS), another type I RIP, was shown to interact with the rat ribosomal stalk proteins (*26*). Systematic deletion and point mutation experiments identified the interaction site on the P protein to the conserved C-terminal tail of P2 and the binding site on TCS to three positively charged amino acids, K173, R174, and K177, in the C-terminal domain (CTD) (*27*). Shiga-like toxin 1 (Stx1) was also shown to interact with human ribosomal proteins P0, P1, and P2 in vitro (*28*). Using deletion mutants of the P proteins, we demonstrated that an intact ribosomal stalk was necessary for RTA to bind to the ribosomes and to depurinate the SRL in vivo (*29*).

The electrostatic character of the ribosomal surface was shown to be responsible for the unusually high catalytic efficiency of the interaction between restrictocin, a fungal ribotoxin, and its target, the SRL (*30*). The electrostatic interactions were also shown to be important for the enzymatic activity of three different RIPs tested, RTA, saporin, and gypsophilin (*31*). The recently determined crystal structure of TCS complexed with the conserved C-terminal peptide of the P-protein confirmed that charge−charge interactions were crucial for the interaction of TCS with this peptide (*32*). Although these studies provide evidence of the importance of the electrostatic interactions in the function of ribotoxins and RIPs, the nature of the catalytic interactions between RIPs and ribosomes has not been well characterized. There is only one report that describes the real-time interaction of RTA with rat ribosomes using surface plasmon resonance (SPR), which proposes a conformational change model (*33*). Here, we used SPR to investigate the interaction of RTA with the wild-type and mutant yeast ribosomes missing an intact stalk. Our results provide evidence of the significant contribution of the stalk to the binding of RTA to ribosomes and demonstrate that RTA interacts with ribosomes via two types of kinetically distinct electrostatic interactions.

MATERIALS AND METHODS

Yeast Strains. The *Saccharomyces cerevisiae* strains that contained deletions in the P proteins were haploid strains, which carried two or four genetic markers depending on different disruptions: D67 (ΔP1) (*RPP1A::LEU2*, *RPP1B::TRP1*), D45 (ΔP2) (*RPP2A::URA3*, *RPP2B::HIS3*) (*34*), and D4567 (ΔP1ΔP2) (*RPP1A::LEU2*, *RPP1B::TRP1*, *RPP2A::URA3*, *RPP2B::HIS3*) (*35*). The wild-type strain was W303 (*MAT*a *ade2-1 trp1-1 ura3-1 leu2-3,112 his-3-11,15 can1-100*). Yeast strains were grown in either YPD medium or minimal SD medium containing 2% glucose.

Monomeric Ribosome Isolation. Salt-washed monomeric yeast ribosome isolation was conducted according to the method of Algire et al. (*36*) with some modifications. The detailed method was described in our previous study (*29*). The concentrations of ribosomes were calculated with the relationship 1 OD_{260} = 20 pmol of ribosomes/mL.

Recombinant RTA. Purified RTA and ricin holotoxin purified from the *R. communis* seeds were obtained from Vector Laboratories (Burlingame, CA). The N-terminal histidine-tagged RTA (molecular mass of 31.6 kDa) was from *Bei*resources (Manassas, VA). The C-terminal histidine-tagged RTA was constructed by cloning the RTA gene into *E. coli* expression vector pET32 (a)+ (Novagen, Madison, WI). This plasmid was transformed into the expression strain, Rosetta-gami (DE3) pLysS, and the expressed RTA was purified using S-tagged agarose. The N-terminal fusion was cleaved by recombinant enterokinase and purified following the manufacturer's protocols. The molecular mass of the purified C-His-tagged RTA was 31.2 kDa. The purity and the concentration of recombinant RTA were determined by a protein assay using the Bio-Rad reagent and by SDS−PAGE followed by both Coomassie blue staining and immunoblotting with polyclonal RTA antibodies. The enzymatic activity of the recombinant RTA was determined by an in vitro depurination and translation inhibition assay (*37*).

In Vitro Translation Inhibition Assay. The Flexi Rabbit Reticulocyte Lysate System from Promega (Madison, WI) was used. The reactions were set up following the Promega protocols. The reaction mixtures were incubated at 30 °C for 30 min. Luciferase activity was measured by using a luminometer. The data were fit with the Slogistic1 equation $Y = a/\{1 + \exp[-k(x - xc)]\}$ using Origin (OriginLab, Northampton, MA). The concentration of RTA that inhibits translation by 50% (IC_{50}) was calculated.

In Vitro Depurination Assay. Twenty picomoles of wild-type ribosomes was incubated with 10 ng of RTA in RIP buffer [60 mM KCl, 10 mM Tris-HCl (pH 7.4), and 10 mM $MgCl_2$] in a total volume of 100 μL at 30 °C for 30 min. Purified RTA from Vector Laboratories and the recombinant RTA from *Bei*resources were used as controls. The depurination activity of the ricin holotoxin was determined after treatment with 30 μM DTT. After incubation of ricin holotoxin with ribosomes, the rRNA was extracted and used for dual-primer extension analysis (*37*).

Analysis of the Interaction between RTA and Ribosomes. The Biacore 3000 (GE Healthcare, Piscataway, NJ) was used to analyze the interaction between the yeast ribosomes and RTA. The N- or C-His-tagged RTA was used as the ligand, and the monomeric ribosomes were used as the analyte. The following equation was used to calculate the theoretical binding signal and the amount of ligand immobilized on the chips: analyte binding capacity (RU) = (analyte MW/ligand MW) × immobilized ligand (RU).

The running buffer consisted of 0.01 M HEPES, 0.15 M NaCl, 50 μM EDTA, 0.005% surfactant P20 (pH 7.4), and 5 mM MgOAc containing different concentrations of KCl. The sensor chips were first washed with the regeneration solution [0.01 M HEPES, 0.15 M NaCl, 0.35 M EDTA, and 0.005% surfactant P20 (pH 8.3)], and then the running buffer containing 500 μM $NiCl_2$ was injected for 1 min to activate the binding site. After the extra washing step, the His-tagged RTA prepared in the running buffer at 50 nM was injected at a flow rate of 20 μL/min to generate a resonance signal of 1500 RU. As a control, the N-terminal His-tagged EGFP (30 nM) prepared in running buffer was immobilized on the reference surface to generate the same RU. Ribosomes were then passed through both the sensor and the reference surfaces at different concentrations at a flow rate of 30 μL/min for 3 min to monitor the association. The dissociation was recorded at the same flow rate for an additional 3 min. The signal from the reference surface was subtracted from the signal from the sensor surface to correct for nonspecific binding. The sensor and the reference surfaces were regenerated by injecting the regeneration solution for 1 min followed by 1 min with a 2 M NaCl solution in running buffer and 1 min with running buffer at a flow rate of 100 μL/min. In every series of ribosome concentration measurements, a buffer sample without ribosomes was injected using the same conditions. The sensorgram generated from the buffer control was subtracted from the sensorgrams obtained at each ribosome concentration to correct for differences due to the sample injection process. Ribosomes were injected at no fewer than five different concentrations for each ribosome preparation at different salt concentrations. All interactions were analyzed at 25 °C. The data were analyzed using BIAevaluation version 4.1. The χ^2 values were within 10% of the maximal binding signal (R_{max}) for each set of kinetic data.

RESULTS

Effect of the Ligand Concentration and the Flow Rate on the Interaction of RTA with Ribosomes. To examine the binding of RTA to the yeast ribosomes by SPR, the His-tagged RTA was immobilized on the NTA chip as the ligand and ribosomes were used in a mobile solution as the analyte. Since the molecular mass of the ribosome (3600 kDa) (*38*) is ~120 times larger than the molecular mass of the N-terminally (31.6 kDa) or C-terminally His-tagged RTA (31.2 kDa), if every immobilized RTA molecule interacted with one ribosome when 1 RU of RTA was immobilized on the chip, 120 RU should be obtained as the ribosome binding signal. However, at ligand concentrations below 500 RU, we could not detect any interaction, suggesting that not every RTA molecule immobilized on the chip may be available to interact with the ribosomes. We observed a nonspecific interaction between ribosomes and the NTA chip when ribosomes were passed over the NTA chip without the immobilized RTA. To minimize this nonspecific interaction, the N-terminally His-tagged enhanced green fluorescent protein (EGFP), which has a molecular mass (28.8 kDa) similar to that of RTA, was used as the control. The N-His-RTA was immobilized on the target surface at 1500 RU, and the N-His EGFP was immobilized on the reference surface at the same RU. The signal obtained from the reference surface was subtracted from the signal obtained from the target surface to correct for nonspecific binding. Under these conditions, we observed the interaction of ribosomes with RTA, but not with EGFP (Figure S1 of the Supporting Information).

The effect of the flow rate on the interaction was examined using eight different flow rates ranging from 5 to 70 μL/min. The initial interaction rate increased as the flow rate increased from 5 to 30 μL/min (data not shown). The rate of interaction did not change when the flow rate was increased to 40 μL/min. However, the interaction rate decreased when flow rates increased above 40 μL/min. On the basis of these results, a ligand concentration of 1500 RU and a flow rate of 30 μL/min were selected for the kinetic analysis of the interaction between RTA and the ribosomes.

The C-Terminus of RTA Has To Be Exposed for RTA To Interact with Ribosomes. To determine if the orientation of RTA on the sensor chip was critical for binding, we used RTA tagged with six histidines either at its N-terminus or at its C-terminus. The C-terminally His-tagged RTA (C-His-RTA) was expressed in *E. coli* and purified, while the N-terminally His-tagged RTA was obtained from *Bei*resources. The purity of both proteins was analyzed by SDS−PAGE followed by Coomassie blue staining and by immunoblot analysis (Figure S2 of the Supporting Information). The IC_{50} of each protein determined using the rabbit reticulocyte lysate in vitro translation inhibition assay was 28, 62, and 58 pM for recombinant C-His-RTA, recombinant N-His-RTA, and RTA purified from castor beans, respectively (Figure S3 of the Supporting Information). Each protein depurinated ribosomes by dual-primer extension analysis (*37*). When C-His-RTA was immobilized on the NTA sensor chip at 1500 RU and yeast ribosomes were passed over this sensor chip as the analyte, we could not detect any interaction between RTA and the ribosomes (Figure 1), even at a ligand concentration of 1800 RU of RTA (data not shown). In contrast, when N-His-RTA was immobilized on the sensor chip as the ligand at 1500 RU, the interaction between RTA and the ribosomes was detected (Figure 1). The interaction signal between the ribosome and N-His-RTA increased when the ribosome concentration was increased from 5 to 20 nM. These results indicate that the C-terminus of RTA has to be exposed to the analyte for the immobilized RTA to interact with ribosomes, suggesting that the C-terminus of RTA is near the ribosome binding site.

There Are Two Types of Interactions between RTA and Wild-Type Ribosomes, but Only One Type of Interaction Exists between RTA and Ribosomes without an Intact Ribosomal Stalk. We have previously shown using SPR

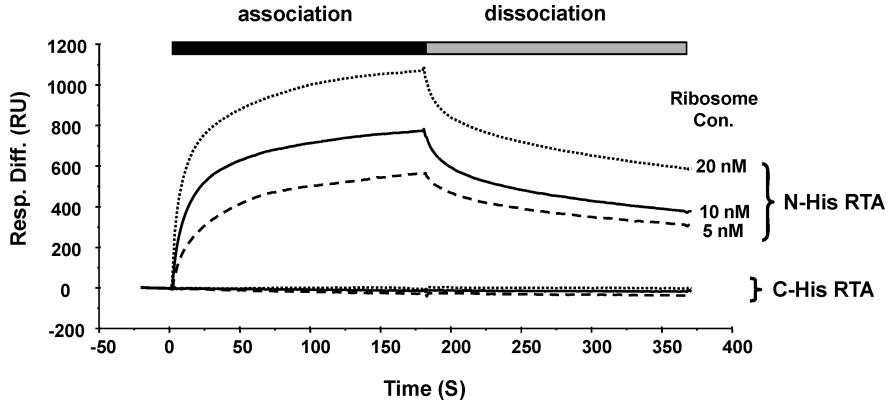

FIGURE 1: Interaction of the N-terminally and C-terminally His-tagged RTA with yeast ribosomes measured by surface plasmon resonance. The N- or C-terminally His-tagged RTA was immobilized on the NTA chip at a concentration of 1500 RU. The N-terminally His-tagged EGFP was immobilized on the reference surface at the same concentration as the control. The salt concentration in the running buffer was 150 mM NaCl. The wild-type ribosomes at 5, 10, or 20 nM were passed over the target surface containing either the N- or C-terminally His-tagged RTA. The signal from the reference surface was subtracted from the signal from the sensor surface to correct for nonspecific binding.

that RTA bound to the wild-type yeast ribosomes. In contrast, very little interaction was observed with ribosomes isolated from the P protein deletion mutants, ΔP1, ΔP2, and ΔP1ΔP2, that did not contain any P1 and P2 proteins (*29*). Only the P0 protein was present on these ribosomes (*34*,*35*). Since previous studies showed that the interaction of RTA with the mutant ribosomes was very weak (*29*), we compared the signal using the wild-type ribosomes at 1 nM and the mutant ribosomes at 7.5 nM (Figure 2). The interaction of RTA with the wild-type ribosomes consisted of a fast association phase during the first 30 s of the association process, followed by a relatively slower association phase. A similar pattern, consisting of a rapid dissociation phase followed by a slower dissociation phase, was also observed during the dissociation process. In contrast, only the slow association and dissociation phases were observed with the mutant ribosomes. Ribosomes from the three different mutants (ΔP1, ΔP2, and ΔP1ΔP2) exhibited similar binding profiles.

To further analyze the interaction of RTA with the wild-type and mutant ribosomes, we conducted a more detailed kinetic analysis by examining the interaction at different ribosome concentrations. The colored lines in Figure 3 represent the experimental data, and the black lines represent the global fitting analysis. As shown in Figure 3A, the interaction between RTA and the wild-type ribosomes was detected when the wild-type ribosomes were used at 0.5 nM. In contrast, the interaction with the mutant ribosomes was detected only when they were used at 5 nM (Figure 3 B−D).

The simulated time courses of the formation and dissociation of the complexes between RTA and the wild-type or mutant ribosomes are shown in Figure 4. Kinetic analysis of the binding data indicated that the interaction of RTA with the wild-type ribosomes did not fit a simple 1:1 binding model but could fit well with the heterogeneous ligand-parallel reaction model. This model predicts two types of interactions between RTA and the wild-type ribosomes: A + B1 ↔ AB1 and A + B2 ↔ AB2. In contrast, the data from the mutant ribosomes fit well with the 1:1 binding model (A + B ↔ AB), indicating that only one type of interaction exists between RTA and the mutant ribosomes. Table 1 shows the association and dissociation rate constants determined from eight different ribosomal concentrations for the wild-type ribosomes and five different ribosomal concentrations for the mutant ribosomes by global fitting. The χ^2 values for each set of kinetic data were within 10% of the R_{max}. The AB1 interaction with the wild-type ribosomes was characterized by a very fast association ($k_{on1} = 1.75 \times 10^7\ M^{-1}\ s^{-1}$) and a very fast dissociation ($k_{off1} = 0.102\ s^{-1}$) rate, while the AB2 interaction was characterized by a much slower association ($k_{on2} = 7.77 \times 10^5\ M^{-1}\ s^{-1}$) and a much slower dissociation rate ($k_{off2} = 1.13 \times 10^{-3}\ s^{-1}$). The AB1 association rate was 23 times faster than the AB2 association rate, while the AB1 dissociation rate was ~90 times faster than the AB2 dissociation rate. Only one type of interaction existed between RTA and the mutant ribosomes, and the association and dissociation rates of the mutant ribosomes were slightly slower than the rates of the AB2 interaction between RTA and wild-type ribosomes (Table 1).

The AB1 Interaction between RTA and the Wild-Type Ribosomes Can Be Saturated with Increasing Ribosome Concentrations. Two types of kinetically distinct interactions existed between RTA and the ribosomes. To determine the relative contribution of each interaction to the total interaction, we examined the simulated time courses of the formation and dissociation of the complexes between RTA and the wild-type ribosomes at different ribosome concentrations (Figure 5). As the concentration of the ribosomes increased, the proportions of the two types of interactions changed. At ribosome concentrations of < 5 nM, the AB1 interaction, which is characterized by the fast association and dissociation rate, was dominant. However, as the ribosome concentration increased to 10 and 20 nM, the AB1 interaction was gradually saturated at ~130 RU and the AB2 interaction, which is characterized by the slower association and dissociation rate, became dominant (Figure 5). These results indicated that the AB1 interaction between RTA and the wild-type ribosomes can be saturated by increasing the ribosome concentration, indicating that this interaction involved a limited number of binding sites.

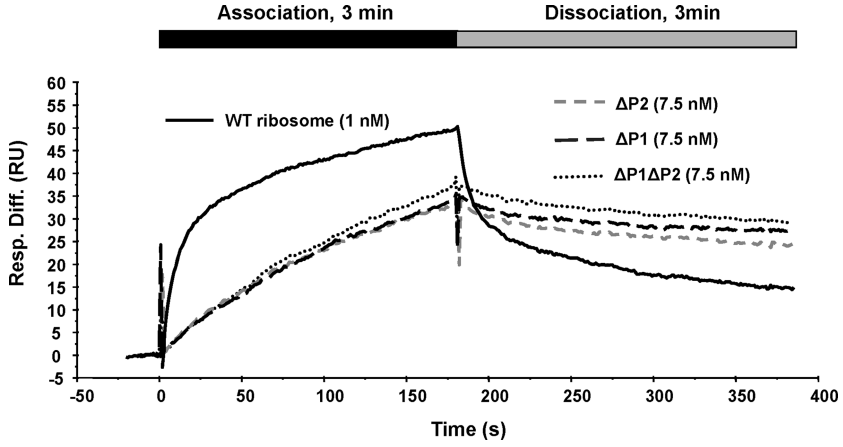

FIGURE 2: Comparison of the interaction of RTA with the wild-type ribosomes and ribosomes from the P protein deletion mutants. The interaction was compared using the wild-type ribosomes at 1 nM and the mutant ribosomes at 7.5 nM. Ribosomes were passed over the target surface containing the N-His-RTA immobilized at 1500 RU and the N-His EGFP immobilized at the same RU as the reference. The salt concentration in the running buffer was 200 mM.

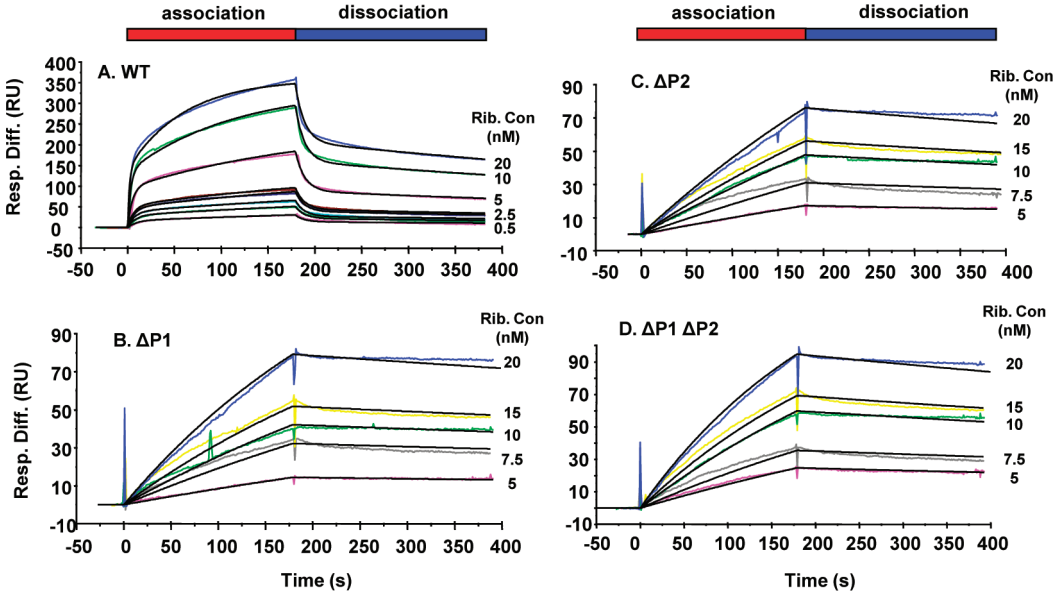

FIGURE 3: Kinetic data and the corresponding global fitting analysis for the interaction of RTA with the wild-type and mutant ribosomes. Varying concentrations of ribosomes indicated on the right were used to obtain the data shown. The scales on the *y*-axes are different between the wild-type ribosomes (A) and the three different P protein mutants (B−D) due to the weaker signal observed with the mutant ribosomes. The colored lines represent the experimental data, and the black lines represent the global fitting analysis. The total salt concentration in the running buffer was 200 mM. The ligand concentration was 1500 RU. The EGFP was immobilized to the reference surface at the same RU as RTA.

The AB2 Interaction between RTA and the Wild-Type Ribosomes Can Be Disrupted at a Relatively Lower Salt Concentration Than the AB1 Interaction. Previous studies indicated that the electrostatic interactions played a major role in the interaction between a ribotoxin and ribosomes (*31*). To determine if electrostatic interactions were important in the interaction between RTA and ribosomes by SPR, we increased the total salt concentration in the running buffer using KCl. As shown in Figure 6, the interaction of RTA with the wild-type or mutant ribosomes weakened dramatically as the total salt concentration increased. The interaction with ribosomes from the ΔP1ΔP2 mutant was almost lost at a salt concentration of 300 mM (green lines in Figure 6B). In contrast, at 300 mM salt there was still some interaction with the wild-type ribosomes (green lines in Figure 6A). The interaction of RTA with the wild-type ribosomes was completely interrupted when the salt concentration was increased to 400 mM (blue lines in Figure 6A).

At a salt concentration of 300 mM, the kinetics of the interaction between RTA and the wild-type ribosomes changed. Kinetic analysis of the binding data indicated that this interaction fit well with the 1:1 binding model (Figure 7). The simulated time courses for the formation and dissociation of complexes at 300 mM salt were similar to the AB1 interaction at 200 mM salt (Figure 5) with a fast association and a relatively fast dissociation rate. As previously observed with the AB1 interaction at 200 mM salt, when the ribosome concentration increased, the binding was also gradually saturated at 300 mM salt (Figure 7). The association and dissociation rates of RTA and the wild-type ribosomes at 300 mM salt ($k_{on} = 5.45 \times 10^6$ M^{-1} s^{-1}, and $k_{off} = 5.82 \times 10^{-3}$ s^{-1})

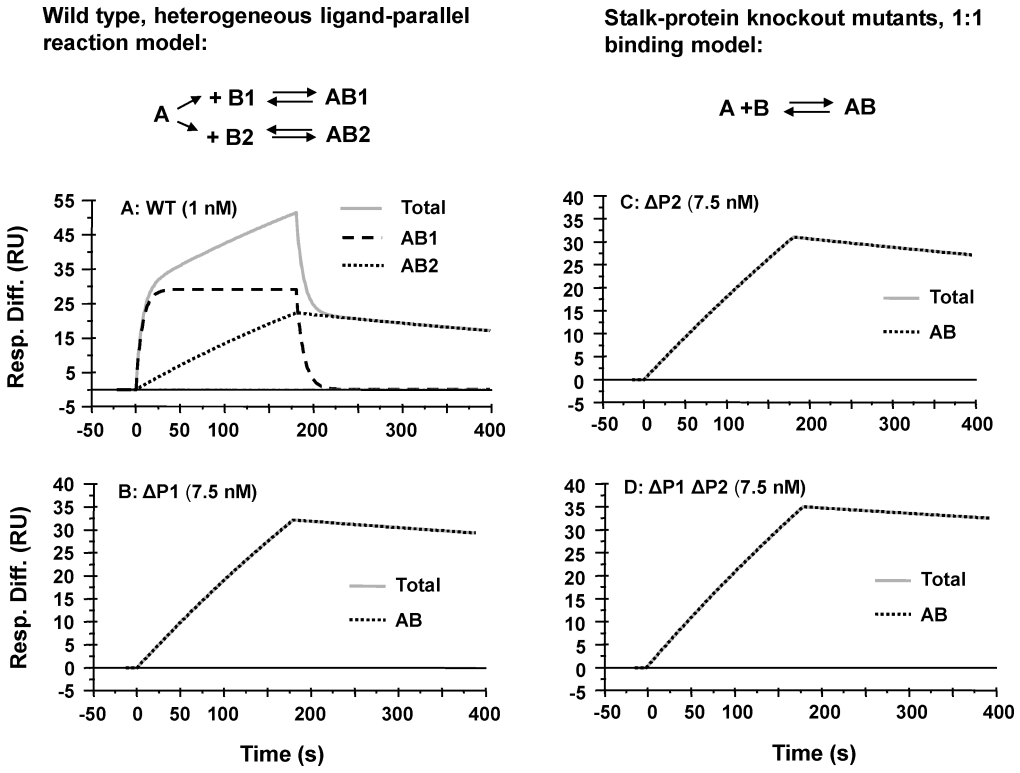

FIGURE 4: Simulated time courses of the formation and dissociation of complexes between RTA and the wild-type or mutant ribosomes. The models correspond to the data shown in Figure 3. The data obtained with the wild-type ribosomes fit best to the heterogeneous ligand-parallel reaction model as shown in panel A. The data with the mutant ribosomes fit best to the 1:1 interaction model as shown in panels B−D. Due to the differences in the interactions between the wild-type and mutant ribosomes, the ribosome concentrations are 1 nM for the wild-type ribosomes and 7.5 nM for the mutant ribosomes.

Table 1: Kinetic Constants (k_{on} and k_{off}) and Calculated Equilibrium Dissociation Constants (K_D) for the Interaction of RTA with the Wild-Type (WT) and Mutant Ribosomes Lacking an Intact Stalk[a]

ribosomes	k_{on1} (M^{-1} s^{-1})	k_{off1} (s^{-1})	K_{D1} (M)	k_{on2} (M^{-1} s^{-1})	k_{off2} (s^{-1})	K_{D2} (M)	R_{max} (average)	χ^2
WT	1.75×10^7 with 200 mM salt	0.102	5.83×10^{-9}	7.77×10^5	1.13×10^{-3}	1.45×10^{-9}	R_{max1} = 196; R_{max2} = 197	12.1 (n = 8)
ΔP1	200 mM salt			8.01×10^4	6.23×10^{-4}	7.78×10^{-9}	317	5.42 (n = 5)
ΔP2	200 mM salt			1.52×10^5	4.42×10^{-4}	2.90×10^{-9}	167	4.87 (n = 5)
ΔPΔP2	200 mM salt			1.95×10^5	5.54×10^{-4}	2.84×10^{-9}	181	4.73 (n = 5)
WT	5.45×10^6 with 300 mM salt	5.82×10^{-3}	1.07×10^{-9}				55	5.35 (n = 12)

[a] The heterogeneous ligand-parallel reaction model was used to fit the data with the wild-type ribosomes at a salt concentration of 200 mM. The 1:1 binding model was used to fit the data with the three different mutant ribosomes at a salt concentration of 200 mM and the wild-type ribosomes at a salt concentration of 300 mM (the last row). Eight to twelve different ribosome concentrations (0.5−20 nM) were used for the wild-type ribosomes and five different concentrations (5−20 nM) for the mutant ribosomes to fit the data to the kinetic models. The χ^2 values for each set of kinetic data were less than 10% of the maximal binding signal (R_{max}).

were slower than the rate of the AB1 interaction at 200 mM salt (k_{on1} = 1.75×10^7 M^{-1} s^{-1}, and k_{off1} = 0.102 s^{-1}) but faster than the rate of AB2 interaction at 200 mM salt (k_{on2} = 7.77×10^5 M^{-1} s^{-1}, and k_{off2} = 1.13×10^{-3} s^{-1}) (Table 1). Since both interactions are dominated by electrostatic interactions, the higher salt concentration is likely to have a negative effect and slow the interactions. Therefore, at 300 mM salt, only the AB1 interaction exists between RTA and the wild-type ribosomes.

We conclude from these results that the interactions between RTA and ribosomes are dominated by electrostatic interactions. The AB1 interaction between RTA and the wild-type ribosomes is stronger than the AB2 interaction. The AB1 interaction is stronger than the interaction between RTA and the mutant ribosomes, and the nature of the AB2 interaction between RTA and the wild-type ribosomes is the same as the nature of the interaction between RTA and the mutant ribosomes.

DISCUSSION

The C-Terminal Domain (CTD) of RTA Is Near the Ribosome Binding Site. The SPR analysis of the interaction between RTA and ribosomes indicated that RTA

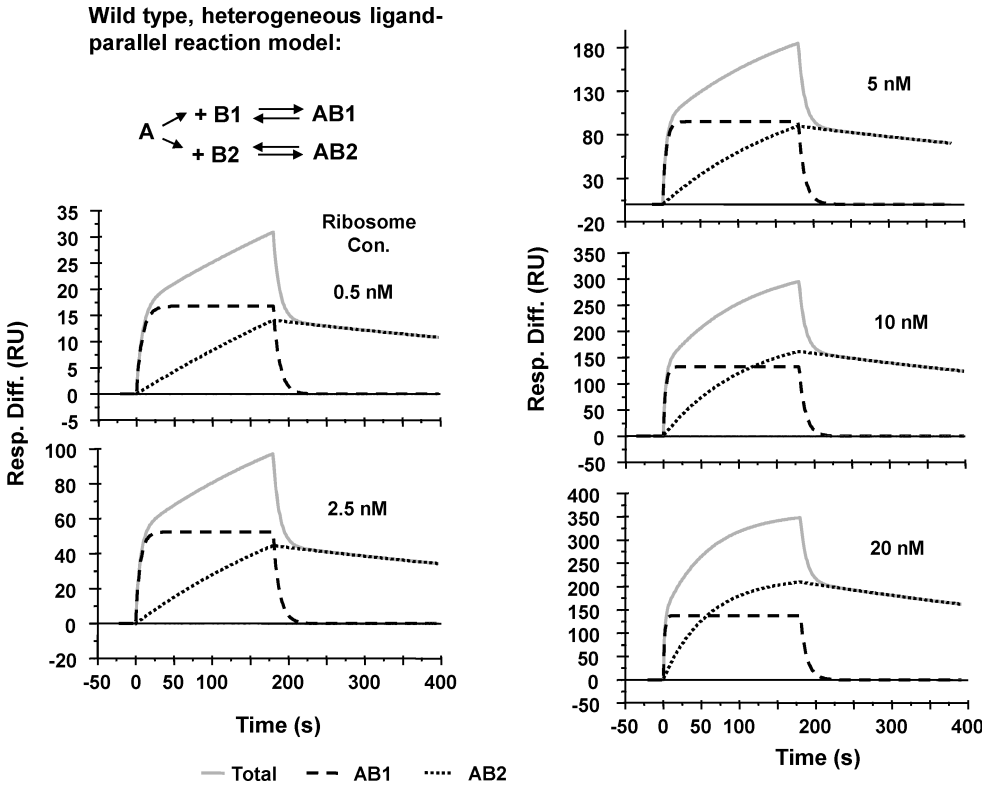

FIGURE 5: Simulated time courses of the formation and dissociation of complexes between RTA and the wild-type ribosomes at different ribosome concentrations. The proportions of AB1 and AB2 in the total binding changed with increasing ribosome concentrations. The AB1 interaction was saturated at a ribosome concentration of 10 nM. The data are from the same data set shown in Figure 3A.

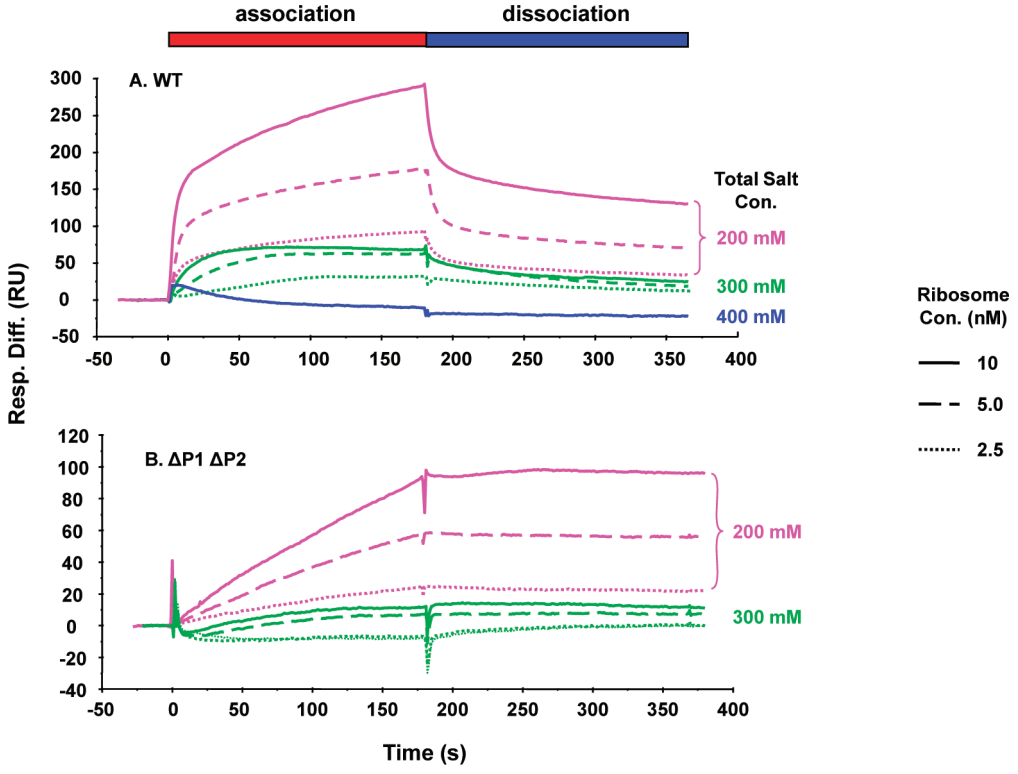

FIGURE 6: Interaction of RTA with the wild-type ribosomes and ribosomes from the P protein mutants at increasing salt concentrations. The interaction of RTA with the wild-type ribosomes was lost at 400 mM salt (A), and the interaction with the mutant ribosomes was almost lost at 300 mM salt (B).

interacted with ribosomes only when its C-terminus was exposed to the analyte (Figure 1). In the crystal structure of RTA, the C-terminus and the N-terminus fold to the opposite sides of the RTA molecule (Figure S4 of the Supporting Information). The C-terminus of RTA is close to the active site, while the N-terminus is far from

the active site (Figure S4 of the Supporting Information). Therefore, when the N-terminus of RTA was immobilized on the chip, the C-terminus and the active site were exposed to the mobile phase. These results indicated that the C-terminus of RTA, which interacts with the B subunit in the holotoxin, is near the ribosome binding site.

Consistent with these observations, the disulfide bond between the A chain and the B chain had to be reduced for the holotoxin to depurinate the yeast ribosomes

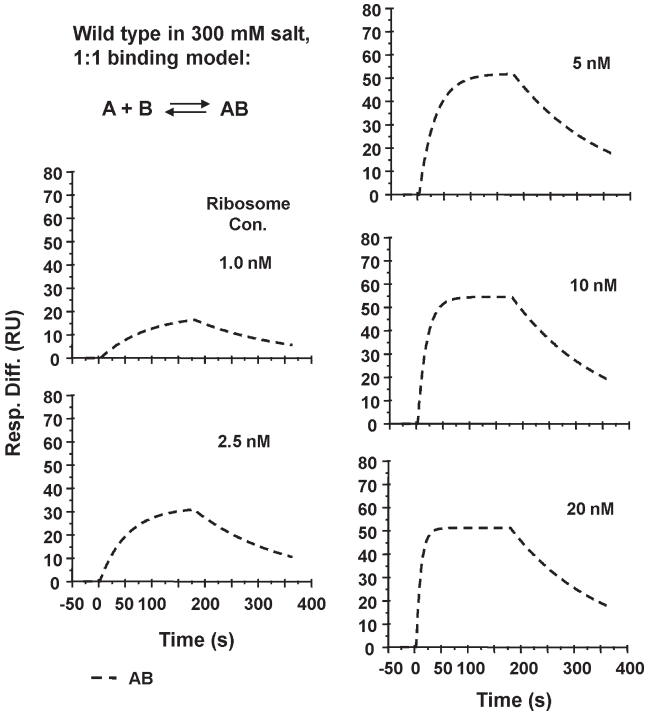

FIGURE 7: Simulated time courses for the formation and dissociation of complexes with the wild-type ribosomes at a salt concentration of 300 mM. The interaction fit the 1:1 binding model and was saturated at a ribosome concentration of 10 nM.

(Figure S5 of the Supporting Information). Early studies indicated that the arginine residues outside the active site cleft were involved in the RTA activity (*39*,*40*). In the X-ray crystal structure of the holotoxin, the B chain docks on the C-terminus of the A chain and the arginine residues in RTA located at the interface are blocked by RTB (Figure 8A). When RTA is separated from RTB, these residues are exposed to the surface and contribute to the positive surface charge at the CTD of RTA (Figure 8B). Since this positively charged region, but not the active site, is blocked by RTB in the holotoxin, the inactivity of holotoxin toward ribosomes may not be due to the lack of interaction with the active site, but possibly due to the blockage of the ribosome interaction site of RTA by RTB (*29*). These results provide evidence that residues outside the active site that are located at the interface between RTA and RTB contribute to the total interaction of RTA with ribosomes.

It is unlikely that ribosome depurination affects the interaction during the SPR measurement. Since, in the Biacore 3000 the flow cell volume is 20 nL and the flow rate used is 30 μL/min, the contact time between RTA and ribosomes is only 40 ms. Therefore, a very small percentage of ribosomes may become depurinated during the SPR measurement. Furthermore, RTA was reported to bind to the depurinated ribosomes in the same pattern as undepurinated ribosomes by SPR, and the interaction of RTA with ribosomes was not inhibited by increasing concentrations of adenine (*33*). Therefore, the interaction analyzed in our study represents the interaction of RTA with ribosomes that are not depurinated, and this interaction occurs between RTA and the stalk and not between RTA and the SRL.

Ribosomal Stalk Specific and Nonspecific Interactions Are Involved in Binding of RTA to Ribosomes, and Both Interactions Are Dominated by Electrostatic Interactions. Our previous studies indicated that RTA bound to the ribosomal stalk, and this binding was required for the

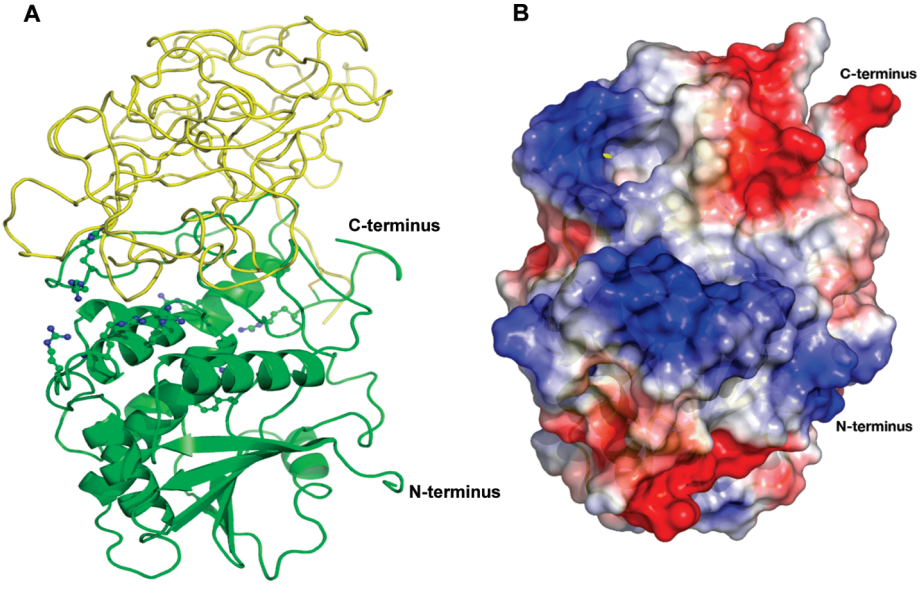

FIGURE 8: Structure of the holotoxin with RTA in a green cartoon model and RTB in a yellow ribbon model (A) and electrostatic potential of RTA (B). The holotoxin structure is from the Protein Data Bank (entry 2AAI) (*43*), and the RTA structure data are from the Protein Data Bank (entry 1IFS) (*44*). This figure was generated using PyMOL. The blue and red represent positive and negative charges, respectively.

depurination of the SRL (*29*). To determine the contribution of the stalk to binding of RTA to the ribosome, we examined the interactions between RTA and the wild-type or mutant ribosomes lacking an intact ribosomal stalk. The kinetic data for the interaction between RTA and the wild-type yeast ribosomes did not fit a simple 1:1 interaction model. Similar results were previously observed between RTA and rat ribosomes by SPR analysis (*33*). In the rat ribosome study, the interaction of RTA with only the wild-type ribosomes was analyzed and a conformational change model was proposed (*33*). When our data for the wild-type and mutant ribosomes were analyzed using the conformational change model, the global fitting results were similar for both types of ribosomes, indicating that this model could not distinguish between the binding of RTA to the wild-type or mutant ribosomes (Figure S6 of the Supporting Information). In contrast, the heterogeneous ligand-parallel reaction model more accurately represented the interaction of RTA with the wild-type ribosomes and could account for the clear differences observed in binding between the wild-type and mutant ribosomes (*29*). This model predicts that either there are two different binding sites on the ribosome or two different types of interactions occur simultaneously with different association and dissociation rates. Fitting our data with this model showed that two types of interactions occurred between RTA and the wild-type ribosomes and only one type of interaction existed between the RTA and the ribosomes without an intact stalk. Here the word "type" was used because each type of binding may involve more than one RTA molecule interacting with a single ribosome. It is possible that several RTA molecules bind to a single ribosome at the same time. Korennykh et al. (*30*) showed that each rat ribosome had ~50 restrictocin binding sites. The AB2 interaction, which may occur between the positively charged CTD of RTA and generally negatively charged ribosomes, is likely a ricin specific, but not a stalk specific, interaction. This type of interaction may involve many binding sites on each ribosome and may serve to concentrate RTA on the ribosomes. The low level of depurination observed in the mutant ribosomes (*29*) might occur only by this nonspecific electrostatic interaction. In contrast, the AB1 interaction is specific and represents binding of RTA to the ribosomal stalk, since this interaction is missing in the mutant ribosomes. The AB1 interaction possibly involves the positively charged CTD of RTA and the negatively charged CTD of the P proteins of the ribosomal stalk. Since there are two P protein heterodimers, P1α/P2β and P2α/P1β on each yeast ribosome, the specific binding sites are limited. Consistent with this, our results indicate that the AB1 interaction can be saturated (Figure 5).

Biochemical studies have shown that the electrostatic interactions contributed to the rapid target localization by restrictocin, one of the ribotoxins that cleave the SRL (*30*). A similar interaction was shown to contribute to ribosome targeting by three different *N*-glycosidases, RTA, saporin, and gypsophilin (*31*). Electrostatic interactions were critical for the interaction of TCS and the human P2 protein by structural analysis (*32*). Our results indicate that the AB1 and AB2 interactions are

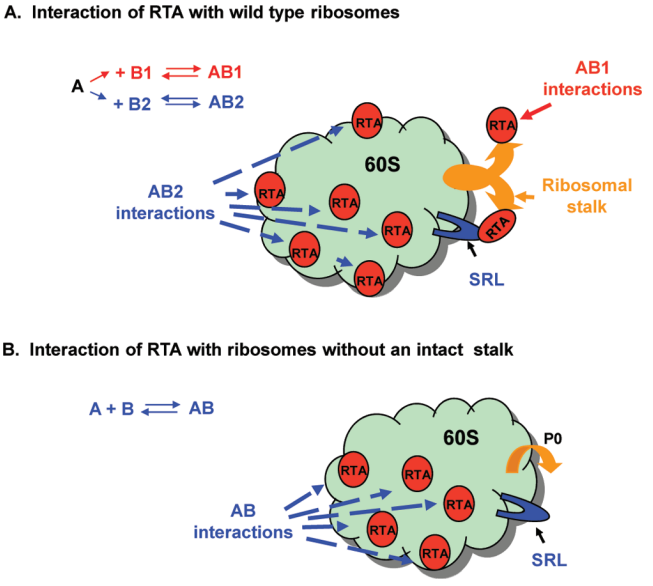

FIGURE 9: Two-step binding model for ribosome depurination by RTA. (A) The slow, stalk nonspecific, electrostatic AB2 interactions concentrate the RTA molecules on the surface of the ribosomes to build up their local concentrations and facilitate the diffusion of RTA toward the stalk, promoting the faster, more specific AB1 interactions between RTA and the stalk. AB1 and AB2 interactions work together on the wild-type ribosomes allowing RTA to localize and depurinate the SRL at a very high rate. (B) Only one type of interaction occurs with the mutant ribosomes deleted in the stalk proteins. The single-step interaction lowers the possibility of a contact between RTA and the SRL, resulting in lower levels of depurination compared to those of the wild-type ribosomes.

dominated by electrostatic interactions, since they are sensitive to the salt concentration (Figure 6). We further show that ionic strength affects the kinetic rates of the AB1 and AB2 interactions. The AB1 interaction is much stronger than the AB2 interaction because a higher salt concentration is needed to disrupt the AB1 interaction than the AB2 interaction (Figure 6).

A Two-Step Binding Model for Ribosome Depurination by RTA. Our results indicate that RTA interacts with ribosomes through two types of kinetically distinct interactions, a saturable, fast interaction that requires an intact stalk and a nonsaturable, slow interaction that does not require an intact stalk. On the basis of these results, we propose a two-step binding model (Figure 9). During the first step, the slow AB2 interactions, which consist of nonspecific electrostatic interactions, concentrate the RTA molecules on the surface of the ribosomes to build up their local concentrations. During the second step, the AB2 interactions facilitate diffusion of RTA toward the stalk and promote the specific AB1 interactions between RTA and the ribosomal stalk. The acidic P proteins of the stalk recruit the RTA molecules that are concentrated on the ribosomes, increasing the rate of association of RTA with the wild-type ribosomes 90-fold over the mutant ribosomes missing the stalk proteins (ΔP1ΔP2) (Table 1). Because of the AB1 interactions, the association and dissociation rates of the AB2 interactions with the wild-type ribosomes are 2−10 times faster than the association and dissociation rates of the interactions with the mutant ribosomes. Therefore, we predict that the AB1 and the AB2 interactions work together allowing RTA to depurinate the SRL at a much higher

rate on the intact ribosomes than on the naked 28S rRNA.

According to this model, the AB1 interaction between RTA and the ribosomal stalk may be similar to the proposed interaction between eukaryotic elongation factor 2 (eEF2) and the ribosomal stalk (*22*). We propose that the CTD of the stalk proteins may bind RTA instead of binding the eEF2 and deliver RTA to the SRL via their flexible hinge region. This is supported by the early studies indicating that ricin inhibits the binding of eEF2 to the ribosome (*41*), eEF2 can protect ribosomes from RTA (*42*), and eEF2 blocks binding of RTA to the ribosome (*8*). The very fast association and dissociation rates between RTA and the ribosomal stalk suggest that RTA may compete with eEF2 for binding to the ribosomal stalk. It has been shown that both TCS (*27*) and Stx1 (*28*) also interact with the ribosomal stalk. Therefore, we predict that the two-step binding model proposed here may be more broadly applicable to the interaction of ribosomes with the other RIPs and with the elongation factors.

ACKNOWLEDGMENT

We thank Dr. Yuan-Ping Pang for making the structure figures, Drs. Arturas Meskauskas and Jonathan Dinman for the ribosome isolation protocol, Dr. Andrew Chow from GE Healthcare for technical support, and *Bei*resources for the N-terminally His-tagged RTA.

SUPPORTING INFORMATION AVAILABLE

Ribosomes interact with RTA but not with EGFP by surface plasmon resonance; purity and activity of the purified recombinant RTA; RTA structure showing the folding of the N- and C-termini of RTA; depurination activity of the ricin holotoxin on yeast ribosomes; and global fitting analysis using the two-state conformational change model. This material is available free of charge via the Internet at http://pubs.acs.org.

REFERENCES

1. Robertus, J. D., and Monzingo, A. F. (2004) The structure of ribosome inactivating proteins. *Mini Rev. Med. Chem. 4*, 477–486.
2. Olsnes, S., and Pihl, A. (1972) Treatment of abrin and ricin with β-mercaptoethanol: Opposite effects on their toxicity in mice and their ability to inhibit protein synthesis in a cell-free system. *FEBS Lett. 28*, 48–50.
3. Olsnes, S., and Pihl, A. (1973) Different biological properties of the two constituent peptide chains of ricin, a toxic protein inhibiting protein synthesis. *Biochemistry 12*, 3121–3126.
4. Olsnes, S., Refsnes, K., and Pihl, A. (1974) Mechanism of action of the toxic lectins abrin and ricin. *Nature 249*, 627–631.
5. Olsnes, S., Fernandez-Puentes, C., Carrasco, L., and Vazquez, D. (1975) Ribosome inactivation by the toxic lectins abrin and ricin. Kinetics of the enzymic activity of the toxin A-chains. *Eur. J. Biochem. 60*, 281–288.
6. Hedblom, M. L., Cawley, D. B., Boguslawski, S., and Houston, L. L. (1978) Binding of ricin A chain to rat liver ribosomes: Relationship to ribosome inactivation. *J. Supramol. Struct. 9*, 253–268.
7. Endo, Y., and Tsurugi, K. (1988) The RNA N-glycosidase activity of ricin A-chain. The characteristics of the enzymatic activity of ricin A-chain with ribosomes and with rRNA. *J. Biol. Chem. 263*, 8735–8739.
8. Cawley, D. B., Hedblom, M. L., and Houston, L. L. (1979) Protection and rescue of ribosomes from the action of ricin A chain. *Biochemistry 18*, 2648–2654.
9. Wool, I. G., Gluck, A., and Endo, Y. (1992) Ribotoxin recognition of ribosomal RNA and a proposal for the mechanism of translocation. *Trends Biochem. Sci. 17*, 266–269.
10. Brigotti, M., Rambelli, F., Zamboni, M., Montanaro, L., and Sperti, S. (1989) Effect of α-sarcin and ribosome-inactivating proteins on the interaction of elongation factors with ribosomes. *Biochem. J. 257*, 723–727.
11. Endo, Y., Chan, Y. L., Lin, A., Tsurugi, K., and Wool, I. G. (1988) The cytotoxins α-sarcin and ricin retain their specificity when tested on a synthetic oligoribonucleotide (35-mer) that mimics a region of 28 S ribosomal ribonucleic acid. *J. Biol. Chem. 263*, 7917–7920.
12. Marchant, A., and Hartley, M. R. (1995) The action of pokeweed antiviral protein and ricin A-chain on mutants in the α-sarcin loop of *Escherichia coli* 23S ribosomal RNA. *J. Mol. Biol. 254*, 848–855.
13. Correll, C. C., Munishkin, A., Chan, Y. L., Ren, Z., Wool, I. G., and Steitz, T. A. (1998) Crystal structure of the ribosomal RNA domain essential for binding elongation factors. *Proc. Natl. Acad. Sci. U.S.A. 95*, 13436–13441.
14. Correll, C. C., Wool, I. G., and Munishkin, A. (1999) The two faces of the *Escherichia coli* 23 S rRNA sarcin/ricin domain: The structure at 1.11 Å resolution.. *J. Mol. Biol. 292*, 275–287.
15. Moazed, D., Robertson, J. M., and Noller, H. F. (1988) Interaction of elongation factors EF-G and EF-Tu with a conserved loop in 23S RNA. *Nature 334*, 362–364.
16. Schuwirth, B. S., Borovinskaya, M. A., Hau, C. W., Zhang, W., Vila-Sanjurjo, A., Holton, J. M., and Cate, J. H. (2005) Structures of the bacterial ribosome at 3.5 Å resolution. *Science 310*, 827–834.
17. Gonzalo, P., and Reboud, J. P. (2003) The puzzling lateral flexible stalk of the ribosome. *Biol. Cell 95*, 179–193.
18. Gudkov, A. T., Tumanova, L. G., Gongadze, G. M., and Bushuev, V. N. (1980) Role of different regions of ribosomal proteins L7 and L10 in their complex formation and in the interaction with the ribosomal 50 S subunit. *FEBS Lett. 109*, 34–38.
19. Griaznova, O., and Traut, R. R. (2000) Deletion of C-terminal residues of *Escherichia coli* ribosomal protein L10 causes the loss of binding of one L7/L12 dimer: Ribosomes with one L7/L12 dimer are active. *Biochemistry 39*, 4075–4081.
20. Bargis-Surgey, P., Lavergne, J. P., Gonzalo, P., Vard, C., Filhol-Cochet, O., and Reboud, J. P. (1999) Interaction of elongation factor eEF-2 with ribosomal P proteins. *Eur. J. Biochem. 262*, 606–611.
21. Savelsbergh, A., Mohr, D., Kothe, U., Wintermeyer, W., and Rodnina, M. V. (2005) Control of phosphate release from elongation factor G by ribosomal protein L7/12. *EMBO J. 24*, 4316–4323.
22. Diaconu, M., Kothe, U., Schlunzen, F., Fischer, N., Harms, J. M., Tonevitsky, A. G., Stark, H., Rodnina, M. V., and Wahl, M. C. (2005) Structural basis for the function of the ribosomal L7/12 stalk in factor binding and GTPase activation. *Cell 121*, 991–1004.
23. Hudak, K. A., Dinman, J. D., and Tumer, N. E. (1999) Pokeweed antiviral protein accesses ribosomes by binding to L3. *J. Biol. Chem. 274*, 3859–3864.
24. Rajamohan, F., Ozer, Z., Mao, C., and Uckun, F. M. (2001) Active center cleft residues of pokeweed antiviral protein mediate its high-affinity binding to the ribosomal protein L3. *Biochemistry 40*, 9104–9114.
25. Vater, C. A., Bartle, L. M., Leszyk, J. D., Lambert, J. M., and Goldmacher, V. S. (1995) Ricin A chain can be chemically cross-linked to the mammalian ribosomal proteins L9 and L10e. *J. Biol. Chem. 270*, 12933–12940.
26. Chan, S. H., Hung, F. S., Chan, D. S., and Shaw, P. C. (2001) Trichosanthin interacts with acidic ribosomal proteins P0 and P1 and mitotic checkpoint protein MAD2B. *Eur. J. Biochem. 268*, 2107–2112.
27. Chan, D. S., Chu, L. O., Lee, K. M., Too, P. H., Ma, K. W., Sze, K. H., Zhu, G., Shaw, P. C., and Wong, K. B. (2007) Interaction between trichosanthin, a ribosome-inactivating protein, and the ribosomal stalk protein P2 by chemical shift perturbation and mutagenesis analyses. *Nucleic Acids Res. 35*, 1660–1672.
28. McCluskey, A. J., Poon, G. M., Bolewska-Pedyczak, E., Srikumar, T., Jeram, S. M., Raught, B., and Gariepy, J. (2008) The catalytic subunit of shiga-like toxin 1 interacts with ribosomal stalk proteins and is inhibited by their conserved C-terminal domain. *J. Mol. Biol. 378*, 375–386.
29. Chiou, J. C., Li, X. P., Remacha, M., Ballesta, J. P., and Tumer, N. E. (2008) The ribosomal stalk is required for ribosome binding, depurination of the rRNA and cytotoxicity of ricin A chain in *Saccharomyces cerevisiae*. *Mol. Microbiol. 70*, 1441–1452.
30. Korennykh, A. V., Piccirilli, J. A., and Correll, C. C. (2006) The electrostatic character of the ribosomal surface enables

extraordinarily rapid target location by ribotoxins. *Nat. Struct. Mol. Biol. 13*, 436–443.
31. Korennykh, A. V., Correll, C. C., and Piccirilli, J. A. (2007) Evidence for the importance of electrostatics in the function of two distinct families of ribosome inactivating toxins. *RNA 13*, 1391–1396.
32. Too, P. H., Ma, M. K., Mak, A. N., Wong, Y. T., Tung, C. K., Zhu, G., Au, S. W., Wong, K. B., and Shaw, P. C. (2008) The C-terminal fragment of the ribosomal P protein complexed to trichosanthin reveals the interaction between the ribosome-inactivating protein and the ribosome. *Nucleic Acids Res. 37*, 602–610.
33. Honjo, E., Watanabe, K., and Tsukamoto, T. (2002) Real-time kinetic analyses of the interaction of ricin toxin A-chain with ribosomes prove a conformational change involved in complex formation. *J. Biochem. 131*, 267–275.
34. Remacha, M., Santos, C., Bermejo, B., Naranda, T., and Ballesta, J. P. (1992) Stable binding of the eukaryotic acidic phosphoproteins to the ribosome is not an absolute requirement for in vivo protein synthesis. *J. Biol. Chem. 267*, 12061–12067.
35. Remacha, M., Jimenez-Diaz, A., Bermejo, B., Rodriguez-Gabriel, M. A., Guarinos, E., and Ballesta, J. P. (1995) Ribosomal acidic phosphoproteins P1 and P2 are not required for cell viability but regulate the pattern of protein expression in *Saccharomyces cerevisiae*. *Mol. Cell. Biol. 15*, 4754–4762.
36. Algire, M. A., Maag, D., Savio, P., Acker, M. G., Tarun, S. Z.Jr., Sachs, A. B., Asano, K., Nielsen, K. H., Olsen, D. S., Phan, L., Hinnebusch, A. G., and Lorsch, J. R. (2002) Development and characterization of a reconstituted yeast translation initiation system. *RNA 8*, 382–397.
37. Parikh, B. A., Coetzer, C., and Tumer, N. E. (2002) Pokeweed antiviral protein regulates the stability of its own mRNA by a mechanism that requires depurination but can be separated from depurination of the α-sarcin/ricin loop of rRNA. *J. Biol. Chem. 277*, 41428–41437.
38. Bielka, H. ((1982)) *The eukaryotic ribosome*, Springer-Verlag, Berlin..
39. Watanabe, K., and Funatsu, G. (1986) Involvement of arginine residues in inhibition of protein synthesis by ricin A-chain. *FEBS Lett. 204*, 219–222.
40. Watanabe, K., Dansako, H., Asada, N., Sakai, M., and Funatsu, G. (1994) Effects of chemical modification of arginine residues outside the active site cleft of ricin A-chain on its RNA N-glycosidase activity for ribosomes. *Biosci., Biotechnol. Biochem. 58*, 716–721.
41. Nolan, R. D., Grasmuk, H., and Drews, J. (1976) The binding of tritiated elongation-factors 1 and 2 to ribosomes from Krebs II mouse ascites-tumor cells. The influence of various antibiotics and toxins. *Eur. J. Biochem. 64*, 69–75.
42. Fernandez-Puentes, C., Benson, S., Olsnes, S., and Pihl, A. (1976) Protective effect of elongation factor 2 on the inactivation of ribosomes by the toxic lectins abrin and ricin. *Eur. J. Biochem. 64*, 437–443.
43. Rutenber, E., Katzin, B. J., Ernst, S., Collins, E. J., Mlsna, D., Ready, M. P., and Robertus, J. D. (1991) Crystallographic refinement of ricin to 2.5 Å. *Proteins 10*, 240–250.
44. Weston, S. A., Tucker, A. D., Thatcher, D. R., Derbyshire, D. J., and Pauptit, R. A. (1994) X-ray structure of recombinant ricin A-chain at 1.8 Å resolution. *J. Mol. Biol. 244*, 410–422.